Environmental Engineering and Management Journal

March 2020, Vol.19, No. 3, 401-410
http://www.eemj.icpm.tuiasi.ro/; http://www.eemj.eu

"Gheorghe Asachi" Technical University of Iasi, Romania

METALLURGICAL WASTE VALORIZATION FOR FABRICATING GLASS-CERAMICS MATERIALS

Erika Iveth Cedillo-González[1,2]*, Juan Jacobo Ruiz-Valdés[2]*, Anabel Alvarez-Méndez[2], Cristina Siligardi[1], Isabella Lancellotti[1]

[1]*Dipartimento di Ingegneria "Enzo Ferrari", Università degli Studi di Modena e Reggio Emilia,*
Via Vivarrelli 10, Modena 41125, Italia
[2]*Universidad Autónoma de Nuevo León, Facultad de Ciencias Químicas, Av. Universidad s/n,*
Ciudad Universitaria, San Nicolás de los Garza 66455, N.L., México

Abstract

The valorization of a metallurgical waste (i.e., an iron-rich slag) as raw material for the fabrication of high hardness glass-ceramics using differential thermal analysis, X-ray diffraction, X-ray fluorescence and scanning electron microscopy was investigated. The melting of the slag was aided by the addition of waste glass cullet (WGC) and the vitrification field of this system was investigated. The non-isothermal crystallization kinetics of the parent glass with the highest slag content was studied by DTA and crystallization of the parent glasses led to of pyroxenic crystalline phases, suggesting the application of the obtained glass-ceramics as building materials. Environmental benefits such as the reduction in the consumption of virgin raw materials and the elimination or reduction of CO_2 and SO_2 emissions due to absence of carbonates and sulphates in the batch composition make it an interesting alternative for the application of this technology.

Key words: CO_2 emission reduction, construction materials, glass-ceramics, metallurgical slag

Received: June, 2013; Revised final: September, 2014; Accepted: October, 2014; Published in final edited form: March, 2020

1. Introduction

Over the past decades the Mexican industrial activity has led to the increase of the pollution levels due to the continuous generation of wastes and their inadequate disposal throughout the Mexican territory (SEMARNAT, 2009). The latest estimation for the generation of hazardous slags wastes in this country reaches 28,086 tons (SEMARNAT, 2012), making necessary the development and application of new technologies to face this problem.

It has been widely documented that the processing of building materials by the recycling and/or reuse of wastes is an interesting approach to solve waste pollution problems (Asokan et al., 2009; Karamanov et al., 2007; Lin, 2007; Ling and Poon, 2012a, 2012b; Marghussian and Maghsoodipoor, 1999; Rambaldi et al., 2010; Schabbach et al., 2012; Simion et al., 2013). Unfortunately, in Mexico industries still disposing wastes in open spaces, where these are subject to atmospheric conditions that could promote their diffusion through the environment.

Since Mexican legislation sets responsibilities and fees for those industries which pollute soil, water and air by the inadequate disposal of wastes (SEGOB, 2009), this research is addressed to the utilization of wastes by fabricating useful and economic glass-ceramics materials that can: (i) fulfill with current legislation; (ii) decrease the quantities of wastes to dispose and (iii) contribute to the protection of the Mexican environment from pollution as consequence of improper waste disposal.

---

* Author to whom all correspondence should be addressed: e-mail: erika.cedillogn@uanl.edu.mx, juan.ruizv@uanl.mx; Phone: +52 81 12556117, +52 81 83294000

Glass-ceramics are fine-grained polycrystalline materials formed by the controlled crystallization of a parent glass of suitable composition (Rawlings et al., 2006). Several types of wastes have been used as starting materials for the glass-ceramics production. Examples include slags and ashes such as blast furnace slags (Francis, 2004, 2005, 2007; Fredericci et al., 2000, 2007; Karamanov et al., 2007; Karamanova et al., 2011; Khater, 2011; Wang et al., 2010; Zhao et al., 2012), steel slags (Karamberi et al., 2007; Khater, 2002; Migliore et al., 2018), copper slags (Marghussian and Maghsoodipoor, 1999), phosphorous slags (Murat et al., 1990), basic-oxygen-furnace slags (Carni et al., 2018; Ferreira et al., 2002), slags from gasification processes (Acosta et al., 2002), incinerator-bottom ash (Karamanov et al., 2014) and rice ash husk (Andreola et al., 2013).

In the present work, the feasibility of forming glass-ceramics from a high-iron content metallurgical slag was investigated. Since this slag is highly refractory, waste glass cullet (WGC) was added to facilitate melting (Francis et al., 2004). As no virgin raw materials were required to obtain the parent glasses, a decrease of the territory consumption is a potential benefit if this technology is applied to obtain glass-ceramics for application in the construction sector. Furthermore, by recycling this waste raw material, SO_2 and CO_2 emissions from the parent glass forming process were reduced or eliminated, since no carbonates or sulphates were added to the batch compositions to introduce Na_2O, CaO and MgO to the glass formulation (Fernández Navarro, 1991).

2. Experimental

The slag used in this study was supplied by a Mexican producer of lead, silver and gold from the northeast of the country. WGC was used to compensate the low content of SiO_2 in the slag and promote its melting at 1450 °C. The chemical composition of both, slag and WGC, using X-ray Fluorescence, XRF (Bruker S4 Pioneer Instrument) was determined. Meanwhile the slag does not present a fixed composition, the average composition is reported here. On the other hand, as the WGC was obtained from recycled soda-lime glass bottles (an industrial standard product), a constant composition was considered. The average chemical composition of the slag (in wt.%) is: 32.91% (Fe_2O_3 + FeO); 18.04% CaO; 17.59% ZnO; 17.38% SiO_2; 5.55% SO_3; 3.16% Al_2O_3; 1.21% PbO; 0.70% MgO and other minor components with percentages of less than 1%. The chemical composition of the WGC (in wt.%) is: 71.15% SiO_2; 14.09% CaO; 12.23% Na_2O; 0.90% Al_2O_3; 0.09% MgO and other minor components with percentages less than 1%.

2.1. Glass formation

The first step of the study involved the investigation of the glass formation ability for the WGC-slag system. This was conducted by melting a first batch formed by 59 wt.% of metallurgical slag and 41 wt.% of WGC. This composition was chosen because it contained 70 wt.% theoretically of network former oxides (NFO) and 25 wt.% of network modifier oxides (NMO). In this work, silica and ferric oxide were considered the principal NFOs (Dingwell and Virgo, 1987; Virgo and Mysen, 1985) while CaO and Na_2O were taken as the principal NMO's. The remaining 5 wt.% corresponded to slag´s impurities. This composition, identified as C41 (41 wt.% of WGC), was formulated with the aim of preventing spontaneous and uncontrolled crystallization of the parent glass during casting.

Since from this first test it was individuated that stable glasses (were "stable glasses" mean glasses that DO NOT present spontaneous and uncontrolled crystallization) could be obtained from mixtures of WGC-slag, several batches with different compositions were prepared. Table 1 shows the theoretical composition of all the batches tested in this work. Furthermore, Table 1 shows the experimental chemical composition of the glasses C41, C50 and C55 determined by XRF. The experimental composition was measured only for these samples since they were considered suitable as parent glasses of glass-ceramics.

Table 1. Theoretical batch compositions and experimental glass compositions (expressed in wt.%). The experimental data was obtained from XRF

	Batches (theoretical)										***Glasses (experimental)***		
	C65	***C60***	***C55***	***C50***	***C41***	***C40***	***C35***	***C30***	***C25***	***C20***	***C55***	***C50***	***C41***
Slag	35	40	45	50	58.6	60	65	70	75	80	45	50	58.6
WGC	65	60	55	50	41.4	40	35	30	25	20	55	50	41.4
SiO_2	52.3	49.6	47	44.3	39.6	38.9	36.2	33.5	30.8	28.1	44.6	40.8	37.8
Fe_2O_3	11.6	13.2	14.9	16.5	19.3	19.8	21.4	23.1	24.7	26.4	17.2	19.8	21.7
CaO	15.5	15.7	15.9	16	16.4	16.5	16.7	16.7	17	17.3	16.2	16.9	16.7
Na_2O	8.0	7.3	6.7	6.1	5.1	4.9	4.3	3.7	3.1	2.5	7.3	6.2	6.0
ZnO	6.2	7.0	7.9	8.8	10.3	10.6	11.4	12.3	13.2	14.1	9.2	10.7	11.7
Al_2O_3	1.7	1.9	2.0	2.1	2.3	2.3	2.4	2.5	2.6	2.7	2.2	2.2	2.5
SO_3	2.1	2.4	2.6	2.9	3.3	3.4	3.7	4.0	4.2	4.5	0.3	0.2	0.1
PbO	0.4	0.5	0.5	0.6	0.7	0.7	0.8	0.9	0.9	1.0	0.6	0.7	0.7
Others	2.2	2.4	2.5	2.7	2.9	2.9	3.1	3.3	3.5	3.5	2.4	2.5	2.8

All the batches were melted at 1450 °C in platinum crucibles for 2 h and then poured on a stainless-steel plate. The "stability" of the quenched materials was evaluated in two steps: (i) visually at the casting moment, i.e., stable glasses did not present spontaneous surface crystallization and (ii) from the temperature difference between the first exothermic peak and the glass transition temperature in the DTA curve ($T_p^{exo} - T_g > 100$ °C for "stable" glasses (Araújo et al., 1999). X-ray diffraction (XRD) and differential thermal analysis (DTA) were used to confirm the presence of glassy state. XRD analysis were carried out in a Siemens D5000 diffractometer with Cu K_α radiation, operated at 35 kV and 25 mA and DTA analysis of the grounded parent glasses (particle size 45 µm) were performed in air in a TA Instrument SDT 2960 using a heating rate of 10 °C/min

2.2. Study of the crystallization kinetics (Glass C41)

The total non-isothermal crystallization (i.e., taking into account both nucleation and crystallization processes) of the glass C41 was investigated to determine the best heat treatment conditions to obtain glass-ceramics. Composition C41 corresponds to the stable glass with the highest slag content and it was chosen to conduct the kinetic study because the goal of this work was obtaining glass-ceramics with the highest possible slag content. The activation energy, E_a was calculated from the Kissinger's equation modified by Bansal (Ray and Day, 1993) (Eq. 1):

$$ln\,(\varphi\,/\,Tp^2) \;=\; ln(\nu) \;-\; ln\,(Ea\,/\,R) - (Ea\,/\,RTp) \quad (1)$$

where φ is the heating rate (°C/min), T_p is the crystallization peak temperature (°C), ν is the frequency factor, E_a is the activation energy and R is the gas constant. The Avrami parameter, n, which is a measure of the dimensionality of the crystalline growth, was calculated using the Augis-Bennett equation (Eq. 2) (Ray and Day, 1993):

$$n \;=\; (2.5/\Delta T)(RTp^2/Ea) \quad (2)$$

where ΔT is the width of the crystallization peak at half maxima. The kinetic parameters from Eqs. (1-2), were investigated by performing DTA experiments of glass samples of 20 ± 0.1 mg in a nitrogen atmosphere at diverse heating rates (1, 5, 10, 15, 20 and 25 °C/min).

In addition, the effect of the particle size over the crystallization process was evaluated by testing four different sizes: ≤ 45 µm, $45 \leq x \leq 150$ µm, $150 \leq x \leq 300$ µm and monoliths (20 ± 0.5 mg). Finally, the maximum nucleation temperature (T_n^{max}) was determined using the Ray and Day (1990) method (Eq. 3). This method correlates the maximum temperature of the crystallization peak (T_p) of the DTA diagram with the formed number of nuclei per unit volume (N):

$$ln\,N \;=\; (mEa/RTp) \;+\; c \quad (3)$$

where m is the crystalline growth dimensionality and c is a constant. Thus, DTA experiments of 20 ± 0.1 mg of glass C41 powders between 150 and 300 µm were made at intervals of 20 °C, beginning from the glass transition temperature (T_g), up to several degrees before the temperature of the first crystallization peak, i.e., the nucleation temperature (T_n). The experiments were carried out in a nitrogen atmosphere with a heating rate of 15 °C/min. Once T_n was reached, samples were nucleated for 2 hours at each nucleation temperature previously chosen (T_n) and heated to reach T_c. The T_n^{max} was then obtained from the graph T_p vs T_n.

2.3. Glass-ceramic fabrication

The thermal treatment for the obtainment of a glass-ceramic from the parent glass C41 (highest slag content) was chosen from the kinetic study: glass pieces were nucleated at 640 °C for 30 min and then crystallized at 810 °C for 90 min, using a heating rate of 15°C/min. After the crystallization stage, quenching in air to preserve the crystalline phases was carried out. Since the objective of this work was the promotion of the re-use of the major quantity possible of slag, the thermal treatments of the glasses with the second highest iron content, i.e., C50 and C55 were based only in their DTA curves.

2.4. Glass and glass-ceramics characterization

Crystalline phases were determined by XRD. The linear expansion and the linear thermal expansion coefficient, (linear TEC, α) of both, parent glasses and glass-ceramics, were determined by dilatometry in the temperature interval of 50 – 400 °C using a heating rate of 5 °C/min (Misura 3.32 Dilatometer, Expert System Solutions) and test pieces of 0.5x0.5x1.3 cm. The elastic properties such as the Young modulus (E), the shear modulus (G) and the Poisson coefficient (ν) were assessed by the Impulse Excitation Technique (Grindosonic Mk5 apparatus, J. W. Lemmens). Vickers micro-hardness of the obtained materials was measured using disc shaped samples, of 1 cm diameter and 4 mm thick (402MVD Wolpert). The samples were indented with a 100g load for 10s. Leaching characteristics of the glass-ceramics were evaluated applying the Standard EN 12457-2 (2002). The concentration of the leached elements was analyzed by Inductively coupled plasma atomic emission spectroscopy (ICP-AES-Thermo Jarrell Ash, Iris Advantage with vaporizer Cetac Technologies U5000AT+). The results of the leaching tests were compared with the limits established by the Mexican standard NOM-052-ECOL-93 (PROFEPA, 1993), which states the characteristics of leachates from hazardous wastes, and also with the Italian D.M. 17/09/2010 (MATTM, 2010) regulation regards non-hazardous waste landfilling.

Finally, the chemical durability of all the materials using the Russian standard GOST 10134-62 (HCl 1N and NaOH 1N for 3h at 96 °C) (Garza-García et al., 2007) and the Japanese standard JISR-3520 (distilled water for 1h at 96 °C) was evaluated.

3. Results and discussion

3.1. Glass formation

Glasses were only obtained from the compositions batches between C30 and C65. From these compositions, the C30, C35 and C40 generated glasses with spontaneous and uncontrollable surface crystallization, although crystals concentration was below 5 wt.% as they were not detected from XRD. Furthermore, these surface crystals did not influence the T_g values of glasses C30, C35 and C40, as can be seen in Fig. 1 (legend SC). The surface crystallization phenomenon was attributed to the high slag content (60 – 70 wt.%) and the consequent relatively high concentration of nucleant agents such as TiO_2, Cr_2O_6, Fe_2O_3, MoO_3 and ZrO_2 (Rawlings et al., 2006) present in these samples. Compositions C41, C50 and C55 generated "stable" glasses that were easy to pour, while the C60, C65 and C70 compositions produced very viscous glasses that was impossible to pour. Finally, the batches with higher slag contents produced materials predominantly amorphous, but with uncontrollable magnetite crystals growth (XRD pattern is not showed here) due to their high iron content.

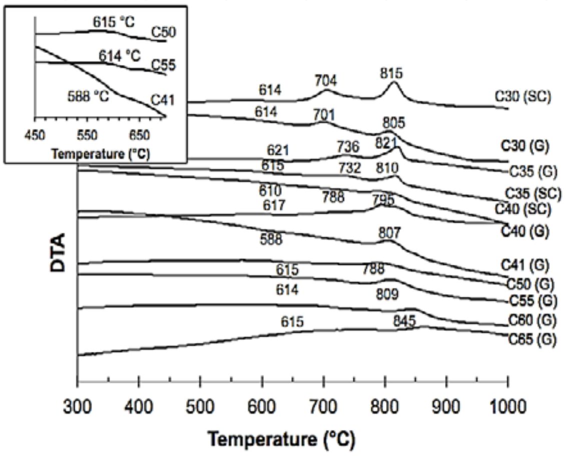

Fig. 1. DTA curves of the obtained glasses. The inset box shows the T_g of the parent glasses C41, C50 and C55. G = glass; SC = surface crystallization

Fig. 1 shows the DTA curves of all the obtained glasses. It can be seen that the glass transition temperature remains practically constant (614 – 621 °C) for all the compositions, except for the glass C41, which has the highest iron content from all the compositions that form "*stable*" glasses. The low T_g value of 588 °C of this glass possibly indicates that in this particular case, the iron is principally in the Fe^{2+} form, acting as a glass network modifier. For the glasses with higher slag content, i.e., higher iron content, the T_g values suggest that the Fe^{3+} form is predominant (very likely acting as glass network former). This hypothesis was confirmed by the location of the glass compositions in the vitrification field of the slag-WGC system presented in Fig. 2. According with Dingwell and Virgo (1987), Kuryaeva (2004) and Virgo and Mysen (1985), Fe^{3+} cations can exhibit either fourfold or sixfold coordination in iron glasses, depending on the content of alkali and alkaline-earth metals. When the concentration of alkali and alkaline-earth metals is low, Fe^{3+} cations exhibit sixfold coordination and they act as network-modifiers. If the amount of alkali and alkaline-earth metals is raised, Fe^{3+} cations act as network formers as they exhibit tetrahedral coordination. In this work, batch C25 is located in the crystal region (i.e., the region where glass formation was not possible) and contents 12.5 mol % of alkaline and alkaline-earth oxides. On the other hand, all the batches that are located in the glass-forming region have an almost constant concentration of alkali and alkaline-earth oxides of ca. 28 mol %. Then, based in the melting tests, it is very likely that Fe^{3+} cations act as network-forming cations due to the relatively high content of alkaline and alkaline-earth oxide content in the prepared glasses.

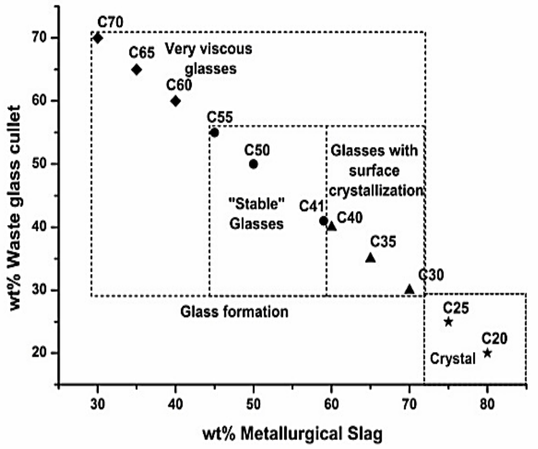

Fig. 2. Vitrification field of the slag-WGC system

3.2. Study of the crystallization kinetics (Glass C41)

Fig. 3 shows the DTA curves of the glass C41 samples treated at different heat rates using three different particle sizes. As it can be seen in Fig. 3, for a constant heating rate, T_p decreases when increasing particle size. Moreover, for a constant particle size, T_p has low values for slow heating rates (10 and 15 °C/min), compared with its values for faster heating rates. The decrease of T_p can be explained by the number of nuclei present at each particle size. It is known that for constant heating rate, T_p depends on the total concentration of surface and bulk nuclei, and decreases with increasing the concentration of these nuclei (Erol et al., 2011). Since the surface area increases when decreasing particle size, the concentration of surface nuclei is expected to be higher for fine particles.

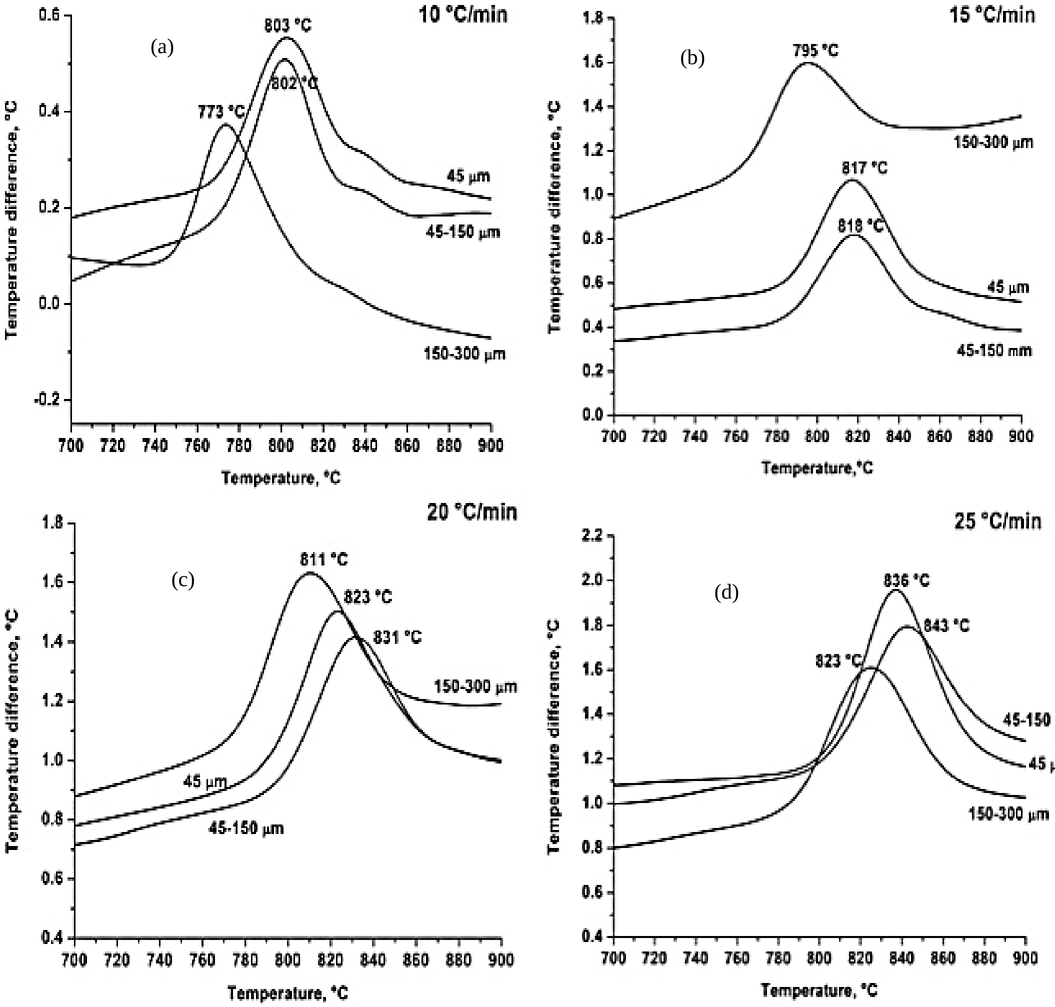

Fig. 3. DTA exotherms of the glass samples at different heating rates and particle sizes. Heating rates: (a) 10 ºC/min; (b) 15 ºc/min; (c) 20 ºC/min and (d) 25 ºC/min

On the other hand, as the particle size increases, the quantity of internal nuclei also increases, because bigger particles provide larger effective volumes for internal nucleation. If the surface crystallization mechanism is dominant, T_p should move to low values when decreasing particle size. However, as it was stated before, in this case T_p shifts to lower values when increasing particle size, indicating possibly that bulk crystallization is the dominant mechanism for this glass, due to the higher quantity of internal nuclei that promotes the bulk crystallization of the glass at lower temperatures.

Regards the change of T_p with the heating rate, if comparing to a given particle size at two different heating rates, for example, 45 µm particles at 10 and 25 °C/min (slow and fast), it can be observed that T_p has a lower value for 10 °C/min. It has been stated that if a glass is not initially saturated with internal nuclei during a DTA scan, their concentration will be higher for slower heating rates, since the glass spends a longer time in the temperature range where nucleation can occur (Erol et al., 2011). This means that T_p should have low values for slow heating rates and high values for fast heating rates, as occurs in these results. Table 2 shows the obtained values of E_a and ν, calculated from the plot of $1/T_p$ vs $\ln(\varphi/T_p^2)$ (Eq. 1) and the Avrami parameter calculated using the Augis-Bennett method (Eq. 2). It can be seen that the E_a value decreases when increasing the particle size. These changes in E_a and the obtained values for n indicates that the crystallization process changes with the particle size.

Table 2. Values of E_a, ν and n obtained for the C41 glass in different treatment conditions

Particle size (µm)	*E_a (kJ·mol^{-1})*	*ν (min^{-1}) X 10^{11}*	*n (Average)*
≤45	297.4 ± 0.01	825 ± 5.00	1.8 ± 0.07
45 ≤ x ≤ 150	260.8 ± 0.01	11.5 ± 0.51	2.2 ± 0.08
150 ≤ x ≤ 300	245.1 ± 0.07	5.5 ± 0.01	2.2 ± 0.06

An analysis of the exotherms in Fig. 3 and (Eq. 2) permitted to explain that the crystallization mechanism changes as the size particle changes. From

(Eq. 2) it can be seen that when increasing the peak width, ΔT, *n* decreases, indicating that the dominant mechanism is the surface crystallization. This phenomenon occurs for small particles, which have a big specific area/volume ratio. For bigger particle sizes, the ΔT decrease leading to *n* higher values; this is related at bulk crystallization. Finally, from the plot T_p vs T_n of the Ray and Day method described in (Eq. 3) (Ray and Day, 1990) a T_n^{max} equal to 640°C was calculated (plot is not shown here).

3.3. Glass-ceramics characterization

Fig. 4 shows that the C50 and C55 glass-ceramics are formed by the same crystalline phases: petedunnite, $CaZn(Si_2O_6)$ (pyroxenes group) and aegirine, $NaFe^{3+}(SiO_3)_2$ (inosilicates group). On the other hand, glass-ceramic C41 is formed by hardystonite, $Ca_2ZnSi_2O_6$ and the $NaFe^{3+}(SiO_3)_2$. At 1085°C, glass-ceramic C41 also contains $ZnFe_2O_4$, which possess magnetic properties. Fig. 5 shows the SEM micrographs of the C41 glass-ceramic, where the microstructure can be observed (crystal size ≈ 1 μm). From EDS, it was determined that glass-ceramic C41 (810 °C) is formed by two types of agglomerates of small particles, a rich in Si and Ca one, attributed at the $Ca_2ZnSi_2O_7$ phase, and another rich in Si and Fe, attributed to the $NaFe^{3+}Si_2O_6$ crystalline phase.

A key parameter of the glass-ceramics used for the fabrication of construction elements such as glazes wall and floor tiles is the linear thermal expansion coefficient (α). This parameter must be similar to that of the conventional supports to avoid the generation of shear stresses by thermal gradients between layers. Table 3 presents the α values for the prepared glasses and glass-ceramics. The value of α decreased on the glasses as the iron content (or the slag content) decreased, while the α values of the glass-ceramics remained practically constant for the three compositions. This can be explained by their crystallographic characteristics, as they are formed by combinations of the same crystalline phases.

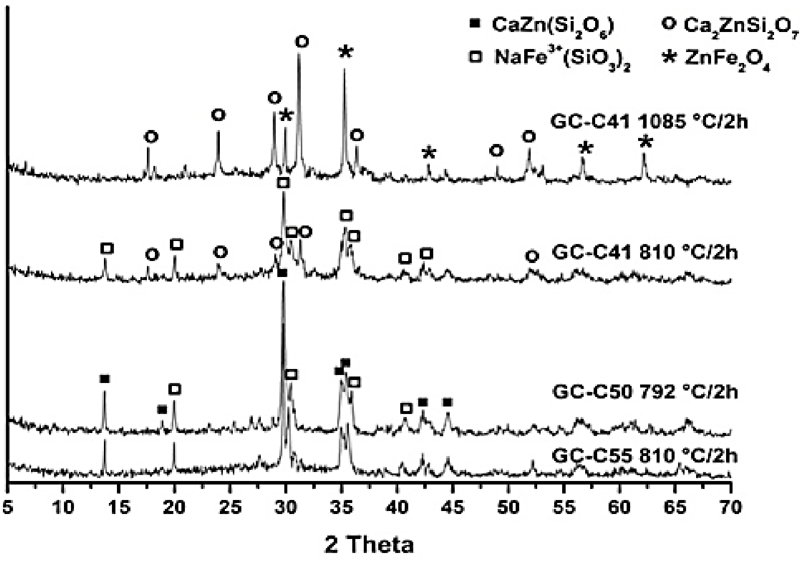

Fig. 4. XRD patterns of the prepared glass-ceramics

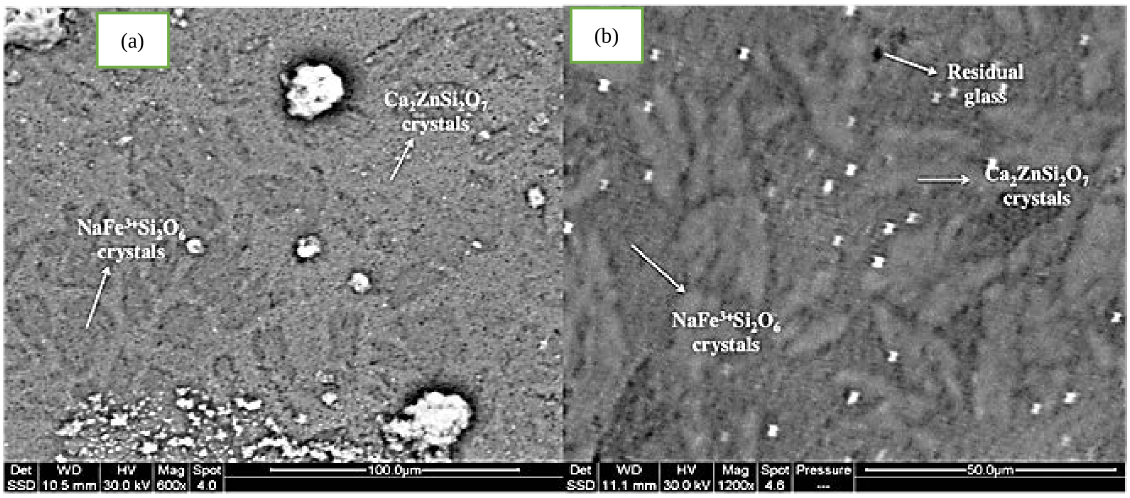

Fig. 5. SEM micrographs of the glass-ceramic C41. (a) Micrograph taken at 600x; (b) Micrograph taken at 1200x

Table 3 also shows the α values of some materials commonly used in the building industry (Institute of Ceramic Promotion, 2009). It can be seen that the α value of the prepared glass-ceramics (6.14 – 6.58 X 10^{-6} °C^{-1}) is similar at those of some kinds of marbles (7 X 10^{-6} °C^{-1}). Table 4 shows the values of the Young modulus (*E*), the shear modulus (*G*) and the Poisson coefficient (*v*) obtained for the glasses and glass-ceramics of the C41 and C50 compositions, as well as for other materials. These parameters could not be determined for the materials generated from composition C55, since the necessary test specimens could not be formed due to its high viscosity. As presented in Table 4, the *E* and *G* values for the prepared glasses are similar to those of the soda-lime glass (Valley Design Corporation, 2015).

In the case of the glass-ceramics, *E* and *G* values are higher than the glasses and soda-lime glass. The values of the Poisson module for the glasses and the glass-ceramics are higher than for the soda-lime glass. Furthermore, from Table 4 it can be inferred that the Young's modulus is higher for the glasses and glass-ceramics than for the brick, concrete, marble and granite, materials widely used in the construction industry. From these results, it was concluded that the glass-ceramics obtained from the investigated slag could be used for the fabrication of floor tiles, due to their values of *E*, higher than the granite and the marble, both natural stones used for the fabrication of floor tiles (Giancoli, 2002).

The Vickers microhardness of the parent glasses of compositions C41, C50 and C55 were 5.27, 5.39 and 5.08 GPa, respectively. These values are higher than that the Vickers microhardness of 4.1. GPa for window glasses (Mazurin et al., 1983). Crystallization of the parent glasses promoted a slightly increase in the Vickers hardness. Hardness values of glass-ceramics with compositions C41, C50 and C55 were 5.32, 5.41 and 5.59 GPa. Although these values are only slightly higher than those of the parent glasses, they are comparable to the reported microhardness of granite (5.5 GPa, (Suzuki and Tanaka, 1997)). Furthermore, the microhardness values of the prepared materials are in good agreement with other glass and glass-ceramics prepared from wastes (Fredericci et al., 2000; Park and Heo, 2002).

Table 5 shows the metal concentrations of the leachates from the glass-ceramics. All the materials release quantities of the investigated metals below the limits set by the Mexican standard NOM-052-ECOL-93 and the Italian regulation D.M. 17/09/2010. According to the last column of Table 5, all the three glass-ceramics obtained here can be used in the Mexican building industry without risk of contamination of soils, since these materials release metals quantities that are way below of the concentration limits for residential soils in Mexico.

Table 6 shows the chemical durability (wt. loss %) of all the glasses and glass-ceramics, as well as the starting materials (slag and WGC) evaluated in aqueous, acid and alkaline media. These tests were carried out with the aim of investigating the environments of application of the final products. For example, an environment where acid rain is a common phenomenon should not be recommended for exterior building materials with low resistance to acids. On the other hand, the same materials can be safely used if they are applied as indoor components or in an environment that is not subject to the influence of acids. Table 6 shows that the metallurgical slag is very susceptible to the acid attack but it is relatively stable in the aqueous and alkaline media due to the presence of metals. These results are in good agreement with those reported by Chiou et al. (2009), as slags were reported to be more affected by acidic than alkaline media.

Table 3. Linear thermal expansion coefficients in the temperature interval from 50 to 100 °

Material	*$\alpha_{50-100°C}$ x 10^{-6}/ °C*	*Material*	*$\alpha_{50-100°C}$ x 10^{-6}/ °C*
Glass C41	8.10 ± 0.01	**Marble**	4.0 – 7.0
Glass C50	5.46 ± 0.07	**Cement mortar**	10.0 – 13.0
Glass C55	4.23 ± 0.03	**Concrete**	10.0 – 13.0
Glass-ceramic C41	6.30 ± 0.01	**Concrete with perlite**	6.0 – 8.0
Glass-ceramic C50	6.58 ± 0.08	**Gypsum**	18.0 – 21.0
Glass-ceramic C55	6.14 ± 0.01		

Table 4. Values of *E, G* and *v*

Material	*E (GPa)*	*G (GPa)*	*v*
Glass C41	77	30	0.30
Glass C50	77	30	0.29
Glass-ceramic C41	116	45	0.29
Glass-ceramic C50	117	45	0.28
Soda-lime glass	72	30	0.22
Brick	14	-	-
Marble	50	-	-
Concrete	20	-	-
Granite	45	-	-

Table 5. Metals release from the glass-ceramics

	Composition			***Limits NOM-052-ECOL-93 (mg/l)***[b]	***Limits D.M. 29/09/2010 (mg/l)***[c]	***Limits residential soil (mg/kg)***[d]
Metal	***C41***	***C50***	***C55***			
Cr	0.015	n.d.[a]	0.004	5.0	1.0	375
Pb	0.003	n.d.[a]	0.031	5.0	1.0	200
Ni	n.d.[a]	0.007	n.d.	5.0	1.0	150
As	0.082	0.088	0.065	5.0	0.2	20

[a] n.d. = not detected; [b] Concentration limit in leachates according to the Mexican standard NOM-052-ECOL-93, which states the characteristics of leachates from hazardous wastes; [c] Concentration limits established by the Italian regulation DM 29/09/2010 for non hazardous waste landfilling [d] Concentration limits in residential soils in Mexico according to PROFEPA (SEMARNAT, 2005)

Table 6. Chemical durability of the starting and prepared materials (wt. loss %)

Sample	***Acid***	***Alkaline***	***Aqueous***
Slag	15.3 ± 0.01	0.2 ± 0.01	1.7 ± 0.05
WGC	4.3 ± 0.01	12.1 ± 0.09	4.4 ± 0.09
Glass C41	5.7 ± 0.05	0.6 ± 0.01	0.7 ± 0.05
Glass C50	5.5 ± 0.05	0.2 ± 0.01	1.2 ± 0.05
Glass C55	3.8 ± 0.01	0.4 ± 0.01	0.7 ± 0.05
Glass-ceramic C41	8.3 ± 0.01	1.2 ± 0.01	1.5 ± 0.01
Glass-ceramic C50	6.5 ± 0.01	1.2 ± 0.03	1.5 ± 0.01
Glass-ceramic C55	5.3 ± 0.02	1.2 ± 0.01	1.5 ± 0.01

In the case of the WGC, it is susceptible to the three modes of chemical attack, being the alkaline attack the most aggressive. Regarding the prepared materials, both the parent glasses and the glass-ceramics are more intensely attacked by the acidic media, while in the aqueous and alkaline media are relatively stables. However, it is clear that as WGC content increases (C41 < C50 < C55), the resistance of both parent glasses and glass-ceramics increases in acidic environment. This behavior was correlated with the increase of the silica content of the batches (see Table 1), since SiO_2 stabilizes the glass network making the final materials stronger. This result was also confirmed by the T_g values shown in the inset box of Fig. 1. Glasses C50 and C55 have higher T_g values than glass C41, suggesting that the glass network is less stable in the last sample. All the presented results in Table 6 indicate that the glasses and glass-ceramics obtained in this work can be only applied in environments where contact with acids (for example, with acidic rain) can be avoided.

3.4. Environmental benefits

Since the glass-ceramics obtained in this work were entirely produced from waste materials, some environmental benefits can be achieved. One of them is the avoiding of the CO_2 release when preparing the parent glasses. For example, production of one ton of parent glass C41 using sand, soda, and limestone requires approximately 87 kg of commercial soda (Na_2CO_3) and 204 kg of commercial limestone ($CaCO_3$) to provide the Na and Ca ions to the glass structure (calculated from raw materials with 99 and 97% purity, respectively). When these materials are heated up at high temperatures, they release CO_2 to form Na_2O and CaO. Therefore, each produced ton of glass C41 from common raw materials, releases 169.8 kg of CO_2 to the environment. Since in both, the slag and the WGC, the CaO and Na_2O are present in an oxidized state, non-extra additions of carbonates are needed and subsequently the emissions of CO_2 are avoided.

Another advantage of the re-use of slag is the improvement of the chemical durability of the final products. As it is observed in Table 6, although all the parent glasses and glass-ceramics exhibit a weight loss in neutral and acidic media, they present lower losses than the “as-received slag”. This characteristic is of great importance when considering the environmental impact of disposed wastes: in Mexico this kind of slags are often disposed in open spaces where they are commonly subjected to atmospheric conditions that can promote leaching and consequently contamination of soils or underground water. If these wastes are transformed in useful glasses and glass-ceramics, the natural waste leaching process can be reduced or avoided (Basegio et al., 2009; Coruh and Ergun, 2006; Kavouras et al., 2003). Finally, an economical benefit involving low costs of production of the parent glasses could be achieved, since all the raw materials are wastes. Furthermore, optimization studies can be conducted to decrease the parent-glasses melting temperature and the optimal nucleation and crystallization times that are required to obtain the final glass-ceramics.

4. Conclusions

Glass-ceramics with pyroxene crystals were obtained from mixtures of slag with 41-55 wt.% of WGC. The properties of the glass-ceramics are similar to those of materials commonly applied in the building industry, so they are suitable for being used as construction elements. The release concentration of potential toxic metals of the final materials is below the limits set by several legislations and they can be thus safely used with a minimal risk of leaching. This can be done only in indoor environments or in those where exposition to acids is negligible. Since only wastes were utilized, reductions in CO_2 emissions of 169.8 kg/ton for glass C41 where achieved.

Acknowledgements

Authors wish to thank to CONACyT for the financial support for this work under the Project No. CB2006/61084 and the CONACyT Beca Mixta (Convocatoria Enero 2009 – Marzo 2010) scholarship.

References

Acosta A., Iglesias I., Aineto M., Romero M., Rincón J., (2002), Thermal and sintering characterization of IGCC slag, *Journal of Thermal Analysis and Calorimimetry*, **67**, 249-255.

Andreola F., Martín M.I., Ferrari A.M., Lancellotti I., Bondioli F., Rincón J.Ma., Romero M., Barbieri L., (2013), Technological properties of glass-ceramic tiles obtained using rice husk ash as silica precursor, *Ceramics International*, **39**, 5427-5435.

Araújo E.B., Eiras J.A., Hernandes A.C., (1999), Studies on tellurite glasses using differential thermal analysis, *Journal of Materials Science Letters*, **18**, 793-795.

Asokan P., Osmani M., Prince A.D.F., (2009), Assessing the recycling potential of glass fibre reinforced plastic waste in concrete and cement composites, *Journal Cleaner Production*, **17**, 821-829.

Basegio T., Beck Leao A.P., Bernanrdes A.M., Bergmann C.P., (2009), Vitrification: An alternative to minimize environmental impact caused by leather industry wastes, *Journal of Hazardous Materials*, **165**, 604-611.

Carni D.L., Lamonaca F., Vitale A., Nastro A., (2018), Measurements to evaluate the possibility to produce bricks from waste cubilot slags, *Environmental Engineering and Management Journal*, **17**, 2329-2335.

Chiou I.-J., Wang K.-S., Tsai C.-C., (2009), Enhancing performance and durability of slag made from incinerator bottom ash and fly ash, *Waste Management*, **29**, 501-505.

Coruh S., Ergun O.N., (2006), Leaching characteristics of cooper flotation waste before and after vitrification, *Journal of Environmental Management*, **81**, 333-338.

Dingwell D.B., Virgo D., (1987), The effect of oxidation state on the viscosity of melts in the system Na_2O-FeO-Fe_2O_3-SiO_2, *Geochimica et Cosmochimica Acta*, **51**, 195-205.

EN 12457-2, (2002), Characterization of waste. Leaching. Compliance test for leaching of granular waste materials and sludge, One stage batch test at a liquid to solid ratio of 10 l/kg for materials with particle size below 4 mm (without or with size reduction), On line at: http://www.sis.se/en/environment-health-protection-safety/wastes/liquid-wastes-sludge/ss-en-12457-2.

Erol M., Kücükbayrak S., Ersoy-Mericboyu A., (2011), Influence of particle size on the crystallization kinetics of glasses produced from wastes materials, *Journal of Non-Crystalline Solids*, **357**, 211-219.

Fernández Navarro J.M., (1991), *Glass*, 2nd Edition (in Spanish), CSIC Press, Madrid, Spain.

Ferreira A.E.B., Zanotto E.D., Scudeller A.M., (2002), Glass and glass-ceramic from basic oxygen furnace (BOF) slag, *Glass Science and Technology*, **75**, 75-86.

Francis A.A., (2004), Conversion of blast furnace slag into new glass-ceramic material, *Journal of European Ceramic Society*, **24**, 2819-2824.

Francis A.A., (2005), Non-isothermal crystallization kinetics of a blast furnace slag, *American Ceramic Society*, **88**, 1859-1863.

Francis A.A., (2007), Magnetic characteristics of iron-containing glass originated from the mixture of various wastes, *Ceramics International*, **33**, 163-168.

Fredericci C., Zanotto E.D., Ziemath E.C., (2000), Crystallization mechanism and properties of a blast furnace slag glass, *Journal of Non-Crystalline Solids*, **273**, 74-75.

Fredericci C., Pizani P.S., Morelli M.R., (2007), Crystallization of blast furnace slag glass melted in SnO_2 crucible, *Journal of Non-Crystalline Solids*, **353**, 4062-4065.

Garza-García M., López-Cuevas J., Gutiérrez-Chavarría C.A., Rendón-Angeles J.C., Valle-Fuentes J.F., (2007), Study of a mixed alkaline-earth effect on some properties of glasses of the CaO-MgO-Al_2O_3-SiO_2 system, *Bolletín de la Sociedad Española de Cerámica y Vidrio*, **46**, 153-162.

Giancoli D.C., (2002), *Temperature and Kinetic Theory*, In: *Physics: Principles with applications*, vol. I, 4th Ed. Prentice Hall Inc., Upper Saddle River. New Jersey, U.S.A.

Institute of Ceramic Promotion, (2009), Coating installation guide: Linear thermal expansion (in Spanish), On line at: http://www.ipc.org.es/guia_colocacion/info_tec_colocacion/los_materiales/baldosas/caract_fis_qui/termica_lineal.html.

Karamanov A., Aloisi M., Pelino M., (2007), Vitrification of cooper flotation waste, *Journal of Hazardous Materials*, **140**, 333-339.

Karamanova E., Avdeev G., Karamanov A., (2011), Ceramics from blast furnace slag, kaolin and quartz, *Journal of European Ceramic Society*, **31**, 989-998.

Karamanov A., Schabbach L.M., Karamanova E., Andreola F., Barbieri L., Ranguelov B., Avdeev G., Lancellotti I., (2014), Sinter-crystallization in air and inert atmospheres of a glass from pre-treated municipal solid waste bottom ashes, *Journal of Non-Crystalline Solids*, **189**, 50-59.

Karamberi A., Orkopolus K., Moutsatsou A., (2007), Synthesis of glass-ceramics using glass cullet and vitrified industrial by-products, *Journal of European Ceramic Society*, **27**, 629-636.

Kavouras P., Kaimakamis G., Ioannidis Th.A., Kehagias Th., Komninou Ph., Kokkou S., Pavlidou E., Antonopoulos I., Sofoniou M., Zouboulis A., Hadjiantoniou C.P., Nouet G., Prakouras A., Karakostas Th., (2003), Vitrification of lead-rich solid ashes from incineration of hazardous industrial wastes, *Waste Management*, **23**, 361-371.

Khater G.A., (2002), The use of Saudi slag for the production of glass-ceramic materials, *Ceramics International*, **28**, 59-67.

Khater G.A., (2011), Influence of Cr_2O_3, LiF, CaF_2 and TiO_2 nucleants on the crystallization behavior and microstructure of glass-ceramics based on blast-furnace slag, *Ceramics International*, **37**, 2193-2199.

Kuryaeva R.G., (2004), Degree of polymerization of aluminosilicate glasses and melts, *Glass Physics and Chemistry*, **30**, 157-166.

Lin K.L., (2007), The effect of heating temperature of thin film transistor liquid crystal display (TFT-LCD) optical waste glass as a partial substitute for clay in eco-brick, *Journal of Cleaner Production*, **15**, 1755-59.

Ling T.C., Poon C.S., (2012a), A comparative study on the feasible use of recycled beverage and CRT funnel glass as fine aggregate in cement mortar, *Journal of Cleaner Production*, **29-30**, 46-52.

Ling T.C., Poon C.S., (2012b), Feasible use of recycled CRT funnel glass as a heavyweight fine aggregate in barite concrete, *Journal of Cleaner Production*, **33**, 42-49.

Marghussian V., Maghsoodipoor A., (1999), Fabrication of unglazed floor tiles containing Iranian cooper slags, *Ceramics International*, **25**, 617-622.

MATTM, (2010), Definition of the criteria for the admissibility of waste in landfills, in place of those contained in the decree of the Minister of the Environment and of the protection of the territory 3 August 2005, Minister of the Environment and of the Protection of the Territory and of the Sea, D.M. 27/09/2010, (in Italian), *Official Journal*, 1-12-2010 n. 281.

Mazurin, O.V., Streltsina, M.V., Shvaiko-Shvaikovskaya, T.P., (1983), *Handbook of Glass Data, Part A*, Elsevier, New York, USA.

Migliore M., Carpinella M., Paganin G., Paolieri F., Talamo C., (2018), Innovative use of scrap and waste deriving from the stone and the construction sector for the manufacturing of bricks. Review of the international scenario and analysis of an Italian case study, *Environmental Engineering and Management Journal*, **17**, 2507-2514.

Murat M., Martel S., Bouster C., (1990), Optimization of devitrification processing in the field of glass-ceramics. Example of the devitrification of phosphorous slag, *Ceramics International*, **16**, 171-175.

Park Y.J., Heo J., (2002), Conversion to glass-ceramics from glasses made by MSW incinerator fly ash for recycling, *Ceramics International*, **28**, 689-694.

PROFEPA, (1993), Official Mexican Standard NOM-052-ECOL-1993, which establishes the characteristics of hazardous waste, listing them and the limits that make a hazardous waste due to its toxicity to the environment, Federal Attorney for Environmental Protection, (in Spanish) On line at: http://www.vertic.org/media/National%20Legislation/Mexico/MX_NOM-052-ECOL-1993.pdf

Rambaldi E., Esposito L., Andreola F., Barbieri L., Lancellotti I., Vassura I., (2010), The recycling of MSWI bottom ash in silicate based ceramic, *Ceramics International*, **36**, 2469-2476.

Rawlings R.D., Wu J.P., Boccaccini A.R., (2006), Glass-ceramics: Their production from wastes, *Journal of Materials Science*, **41**, 733-761.

Ray C.S., Day D.E., (1990), Determining the nucleation rate curve for lithium disilicate glass by differential thermal analysis, *Journal of American Ceramic Society*, **73**, 439-442.

Ray C.S., Day D.E., (1993), Nucleation and Crystallization in glasses as determined by DTA, *Ceramic Transations*, **30**, 207-223.

Schabbach L.M., Andreola F., Barbieri L., Lancellotti I., Karamanova E., Ranguelov B., Karamanov A., (2012), Post-treated incinerator bottom ash as alternative raw material for ceramic manufacturing, *Journal of the European Ceramic Society*, **32**, 2843-2852.

SEGOB, (2009), Agreement that modifies and adds the previous one, by means of which the instructions and format of the Annual Operation Certificate for the Annual Report of the Pollutant Release and Transfer Registry are disclosed, Ministry of the Interior, DOF 5 February 2009, (in Spanish), On line at: http://dof.gob.mx/nota_detalle_popup.php?codigo=5079524

SEMARNAT, (2005), Annual Activities Report 2005, Evaluation of remediation technologies for soils contaminated with metals. Stage II, Ministry of Environment and Natural Resources, (in Spanish), On line at: http://www2.inecc.gob.mx/dgcenica/descargas/metales_ei2004.pdf

SEMARNAT, (2009), The environment in Mexico in 2009, In summary, Ministry of Environment and Natural Resources (in Spanish), On line at: http://app1.semarnat.gob.mx/dgeia/resumen_2009/index.html

SEMARNAT, (2012), Compendium of Environmental Statistics 2012, Ministry of Environment and Natural Resources (in Spanish), On line at: http://app1.semarnat.gob.mx/dgeia/Compendio_2012/index.html

Suzuki S., Tanaka M., (1997), Glass-ceramic from sewage sludge ash, *Journal of Materials Science*, **32**, 1775-1779.

Simion I.M., Ghinea C., Maxineasa S.G., Taranu N., Bonoli A., Gavrilescu M., (2013), Ecological footprint applied in the assessment of construction and demolition waste integrated management, *Environmental Engineering and Management Journal*, **12**, 779-788.

Valley Design Corporation, (2015), Soda-lime float glass properties, On line at: http://www.valleydesign.com/sodalime.htm.

Virgo D., Mysen B.O., (1985), The structural state of iron in oxidized versus reduced glasses at 1 atm: a ^{57}Fe Mössbauer study, *Physics and Chemistry of Minerals*, **12**, 65-67.

Wang Z., Ni W., Li K., Huang X., Zhu L., (2010), Crystallization behavior of glass-ceramics prepared from the mixture of nickel slag, blast furnace slag and quartz sand, *Journal of Non-Crystalline Solids*, **356**, 1554-1558.

Zhao Y., Chen D., Bi Y., Long M., (2012), Preparation of low-cost glass-ceramics from molten blast furnace slag, *Ceramics International*, **38**, 2495-2500.